

Effect of the haeme oxygenase-1/endogenous carbon monoxide system on atherosclerotic plaque formation in rabbits

DA-NAN LIU, YING FANG, LI-RONG WU, XING-DE LIU, PING LI, ZUO-YUN HE

Summary

Objective: To investigate the effect of the haeme oxygenase-1/carbon monoxide (HO-1/CO) system on atherosclerotic plaque formation and its possible mechanism.

Methods: For 12 weeks, rabbits were given a 1.5% cholesterol diet (Ch group, $n = 8$) or a 1.5% cholesterol diet plus an HO-1 inducer, haemin (Hm group, $n = 8$), or an HO-1 inhibitor, zinc protoporphyrin IX (Znpp-IX, Zn group, $n = 8$) by intraperitoneal injection.

Results: Compared with the normal control group (C group, $n = 8$), serum levels of lipids and oxidised low-density lipoproteins (ox-LDL) increased significantly in all experimental groups ($p < 0.01$). However, no significant differences were observed among the three experimental groups ($p > 0.01$). Compared with the control group, aortic nitric oxide (NO) production and nitric oxide synthase (cNOS) activity decreased markedly, whereas carbon monoxide (CO) production and HO-1 activity increased markedly in the Ch group ($p < 0.01$). This was associated with an increase in the area of aortic plaque of $54.00 \pm 4.16\%$. Compared with the Ch group, CO production and HO-1 activity increased markedly, while aortic HO activity and CO production decreased significantly in the Hm group. The area of aortic plaque was significantly reduced in the Hm group ($17.88 \pm 3.01\%$), whereas the area of aortic plaque was significantly increased in the Zn group ($61.13 \pm 3.50\%$). Compared with the Ch group, aortic endothelin-1 expression in the Hm group reduced significantly, while in the Zn group it was significantly higher than in the Ch group ($p < 0.01$).

Conclusion: The HO-1/CO system plays an inhibitory role in atherosclerotic plaque formation. This role was not mediated by regulating serum lipids and ox-LDL, but was related to the reciprocal relationship between the HO-1/CO and NOS/NO systems in atherosclerosis and the down-regulated expression of endothelin-1 (ET-1), which inhibits the proliferation of vascular smooth muscle cells.

Keywords: atherosclerosis, carbon monoxide, nitric oxide synthase, haeme oxygenase

Submitted 2/9/09, accepted 10/3/10

Cardiovasc J Afr 2010; 21: 257–262

www.cvja.co.za

DOI: CVJ-21.001

Endogenous carbon monoxide (CO) is produced from the oxidation of haemoglobin by haeme oxygenase (HO). CO is considered an important messenger molecule, with a similar effect on cardiovascular function as nitric oxide (NO). It activates soluble guanylate cyclase (sGC) and increases cGMP levels, thereby relaxing vascular smooth muscle and inhibiting platelet aggregation and smooth muscle cell proliferation.^{1–4} Some studies have shown that the HO/CO system plays an important role in the inhibition of atherosclerotic plaque formation. However, the specific mechanism and targets are unclear.

In our present study, NOS activity, HO-1 and endothelin-1 (ET-1) expression and the production of NO and CO were evaluated in normal control rabbits, rabbits fed a diet high in cholesterol, those not treated and those treated for 12 weeks with either haemin (an HO inducer) or zinc protoporphyrin IX (an HO inhibitor) in order to investigate the effects of the HO-1/CO system on atherosclerotic plaque formation and its regulatory mechanism.

Methods

The animal centre of Xinqiao Hospital provided 32 New Zealand white rabbits weighing 1.6 to 2.0 kg. The experiment was started after one week of adaptive feeding. The rabbits were randomly divided into four groups: a cholesterol group ($n = 8$, Ch group), a haeme group ($n = 8$, Hm group), a zinc protoporphyrin IX (Znpp-IX) group ($n = 8$, Zn group) and a normal control group ($n = 8$, C group). The rabbits in the C group were fed a normal diet and those in the Ch group were fed a diet containing 1.5% cholesterol. The rabbits in the Hm and Zn groups were fed a high-cholesterol diet, plus haemin (an HO inducer, $15 \text{ mg} \cdot \text{kg}^{-1} \cdot \text{d}^{-1}$) in the Hm group, or zinc protoporphyrin IX (an HO inhibitor, $45 \text{ } \mu\text{mol} \cdot \text{kg}^{-1}$) in the Zn group for 12 weeks by intraperitoneal injection daily.

Blood samples were collected via the ear vein after 12 hours of fasting and aortic tissue was harvested as described below. Cholesterol powder (chemically pure) was imported from the Netherlands and sub-packaged in Guangzhou. Haemin and Znpp-IX were purchased from Sigma (USA). All procedures were performed in accordance with the animal care guidelines of Guiyang Medical College, which conform to the National Institutes of Health Guide for the Care and Use of Laboratory Animals. The ethics committee of our college also approved this study.

Preparation of aortic samples

At the end of the 12th week, all rabbits were anaesthetised by injection of 3% pentobarbital sodium (30 mg/kg) via the ear

Department of Cardiology, Affiliated Hospital, Guiyang Medical College, Guiyang, China

DA-NAN LIU, MD, yi_yi0809@126.com
YING FANG, MD
LI-RONG WU, MD
XING-DE LIU, MD
PING LI, MD

Department of Cardiology, Xinqiao Hospital, Third Military Medical University, Chongqing, China

ZUO-YUN HE, MD

vein and a thoracotomy was immediately performed under sterile conditions. After sampling, all rabbits were sacrificed using an overdose of pentobarbital sodium (Euthanase®) via the ear vein.

The whole aorta was separated, clamped, and then 2 cm was harvested at the lower end of the aortic arch. The connective tissue of the outer membrane was removed and part of the aortic tissue was fixed in 4% paraformaldehyde phosphate buffer for hematoxylin and eosin (HE) staining. Another 3 cm of aorta was fixed in 10% paraformaldehyde phosphate buffer for oil red O staining. Conventional paraffin sections were made and HE staining for light microscopy was done. The remaining fresh tissue samples were kept for the detection of endogenous CO content, NOS activity as well as mRNA expression of HO-1 and ET-1.

After fixation in 10% neutral formalin buffer and conventional dehydration, the aorta was stained with oil red O staining (plaque shows red). The plaque area and aortic tunica-intima area were measured with Leica Qwin image analysis software, and the percentage of the plaque area relative to the aortic tunica-intima area was calculated.

Assays

Serum lipid levels [total cholesterol (TC), triglycerides (TG), high-density lipoprotein cholesterol (HDL-C) and low-density lipoprotein cholesterol (LDL-C)] were determined with an enzymatic kit from the Shanghai Kehua Bio-engineering Co, Ltd (Shanghai, China). The oxidised LDL (ox-LDL) level was determined with the double antibody sandwich method using a kit provided by Shanghai Rongsheng biological reagents factory (Shanghai, China).

A homogenate of blood plasma and aortic tissue was prepared and ET-1 was detected using a radioimmunoassay kit from the Beijing Huaying Biotechnology Co (Beijing, China).

According to the literature,² 500 µl of serum was centrifuged at 10 000 rpm at 4°C for 15 min. A 100-µl volume of the supernatant was removed and 100 µl Griess reagent and 100 µl of 4 mol/l hydrochloric acid were added. The mixture was incubated at room temperature for 10 min and the optical density was read at 570 nm with a microplate reader. A standard curve was prepared using nitrite, and from this curve, serum NO levels were determined.

Detection of aortic NO and CO contents

The aortic smooth muscle was shaved into 3-mm pieces, rinsed with 0.01 mol/l phosphate buffer (pH 7.4) and the sample was added to 2 ml of phosphate buffer for homogenate preparation. The nitrite content (NO₂⁻) in the aortic homogenate, representing NO production was determined with the Greiss method.⁵ CO production was determined according to the method of Morita *et al.*⁶

The smooth muscle of the aorta thoracalis was shaved into 3-mm pieces, placed into 2 ml DMEM medium (15 mg/ml) containing 50 µl/l of haemoglobin (Hb) and incubated at 37°C in a 95% O₂ and 5% CO₂ atmosphere for 2 h.

Relative amounts of CO released into the medium were measured by adding Hb for the last hour of incubation and quantifying carboxyhaemoglobin (HbCO) levels spectrophotometrically using a CO-oximeter (Coming 270; Ciba Coming Diagnostics, Medfield, MA). HbCO gives maximal absorbance at a wavelength of 569 nm and is calculated as percentage total Hb. The

actual amount of Hb was determined from a standard curve using exogenous CO and varying amounts of Hb over a range of concentrations where the absorbance was linear.

Aortic NOS activity was detected by calculating the concentration of ³H-citrulline converted from ³H-arginine.⁷

Protein expression of aortic HO-1 and ET-1 was detected by immunohistochemistry. Goat anti-rabbit HO-1 and ET-1 polyclonal antibodies were purchased from Santa Cruz, USA. An SP-9001 immunohistochemical staining kit was purchased from Zhongshan Goldenbridge Biotechnology Co, Ltd. The percentage area of positive cells was calculated with Leica Qwin image analysis software. Brown vessel wall cells were considered positive for HO-1 or ET-1.

mRNA expression of aortic HO-1 and ET-1

The mRNA expression of aortic HO-1 and ET-1 was determined by RT-PCR. Total RNA was extracted from the aorta using Trizol reagent (Roche, Germany). After determination of purity and concentration, cDNA was generated from total RNA under the following conditions: 50°C for 30 min, followed by 99°C for 5 min and 5°C for 5 min. Then the PCR reaction was performed (RT-PCR kit was purchased from TaKaRa, Japan).

Rabbit HO-1 and ET-1 primers and β-actin gene sequence were obtained according to GenBank (<http://www.ncbi.nlm.nih.gov/>). Primers were designed using DNASIS software (Hitachi Software Engineering Co, Ltd) and synthesised by Shanghai Boya Biotechnology Co. The primers for HO-1 cDNA amplification were as follows: sense: 5'-CAGGTGACTGCCGAGGGTTTA-3'; antisense: 5'-GGAAGTAGA GCGGGCGTAG-3'. The size of the target fragment was 118bp.

The primers for ET-1 cDNA amplification were as follows: sense: 5'-AAGATCCCAGCCAGC ATGGAGAGCG-3'; antisense: 5'-CGTTGCTCCTGCTCCTCC TTGATGG-3'. The size of target fragment was 543bp.

The primers for β-actin cDNA amplification were as follows: sense: 5'-CCCATCTACGAGGGCTACGC -3'; antisense: 5'-CAGGAAGGA GG GCTGGAACA-3'. The size of target fragment was 312bp. β-actin served as the inner control.

The PCR conditions were as follows: HO-1: pre-denaturation at 94°C for 2 min; denaturation at 94°C for 30 s, annealing at 55°C for 30 s, extension at 72°C for 30 s with 32 cycles, followed by a final extension at 72°C for 5 min. ET-1: pre-denaturation at 94°C for 3 min; denaturation at 94°C for 1 min, annealing at 60°C for min, extension at 72°C for 3 min with 30 cycles, followed by a final extension at 72°C for 7 min.

A 10-µl volume of the PCR product was separated with 2% agarose gel. A densitometric scan was performed with the ChemiImager™ 5500 gel imaging machine (Alpha Innotech, USA). The mRNA expression was presented as the integral optical density ratio of HO-1/β-actin and ET-1/β-actin.

Statistical analysis

All data were expressed as mean ± SD. One-way ANOVA was used for comparison among multiple groups.

Results

At the end of the experiment, compared to the control group, serum TC, TG, LDL-C and ox-LDL levels in each high-choles-

terol diet group were significantly increased (all $p < 0.01$), but the increase in HDL-C levels was not significant ($p > 0.05$). Serum TC, TG, LDL-C and ox-LDL levels were not significantly different among all three experimental groups (Table 1).

Compared with the C group, the levels of serum NO in all three experimental groups were significantly decreased (all $p < 0.01$). The levels of serum NO among these three groups were not significantly different (Table 1).

Compared with the C group, the ET-1 content in the blood plasma and aortic tissue in all three experimental groups was significantly increased (all $p < 0.01$). Compared with the Ch group, the ET-1 content in the Hm group was significantly decreased and that in the Zn group was significantly increased (all $p < 0.01$) (Tables 1, 2).

There was no atheromatous plaque in the rabbit aortic tunica-intima in the C group. The plaque area in the Ch, Hm and Zn groups was $54.00 \pm 4.16\%$, $17.88 \pm 3.01\%$ and $61.13 \pm 3.50\%$, respectively. Compared with the Ch group, the plaque area in the Hm group was significantly decreased ($p < 0.01$), but that in the Zn group was significantly increased ($p < 0.01$).

In the C group (Fig. 1), the single-layer endodermis on the luminal surface was intact and the smooth muscle layer was regularly arranged. In the Zn group, the endothelium was damaged and the tunica-intima was significantly thickened with 11 to 12 layers of foam cells. The smooth muscle layer was disorganised and extended to the tunica-intima, with significant atrophy. In the Ch group, endothelial cells were extensively damaged. The tunica-intima was thickened, with eight to nine layers of foam cells, while the degree of smooth muscle atrophy was less than in the Zn group. In the Hm group, the tunica-intima was complete, with occasional foam cells.

Production of aortic NO and CO and NOS activity

Compared with the C group, the production of NO in the Ch group reduced by 27% and the production of CO increased by 55%. cNOS activity decreased by 44%, and iNOS activity increased by 48% (all $p < 0.01$). In the Hm group, the production of NO reduced by 28%, and the production of CO increased by 119%. cNOS activity decreased by 43%, and iNOS activity increased by 24% (all $p < 0.01$). In the Zn group, the production of NO and CO reduced by 26 and 54%, respectively. cNOS activity decreased by 44%, and iNOS activity increased by 74%

(all $p < 0.01$).

Compared with the Ch group, the production of CO significantly increased in the Hm group, and iNOS activity significantly decreased (all $p < 0.01$). The production of NO and cNOS activity were not significantly different between these two groups. The production of CO was significantly decreased, and iNOS activity was significantly increased in the Zn group (all $p < 0.01$). The production of NO, and cNOS activity were not significantly different between these two groups (Table 2).

Expression of HO-1 and ET-1 in aortic tissue

As shown in Figs 2 and 4, HO-1 was mainly expressed in the aortic endothelial cells, foam cells and smooth muscle cells. In the C group, a small number of positive cells were distributed in the tunica-intima. HO-1 was expressed in the endothelial cells. In the Zn group, there were only a few positive cells, and HO-1 was occasionally expressed in the endothelial and foam cells in plaques. The expression rate of HO-1 was significantly lower than in the C group (14.15 ± 1.12 vs $19.02 \pm 1.28\%$, $p < 0.01$).

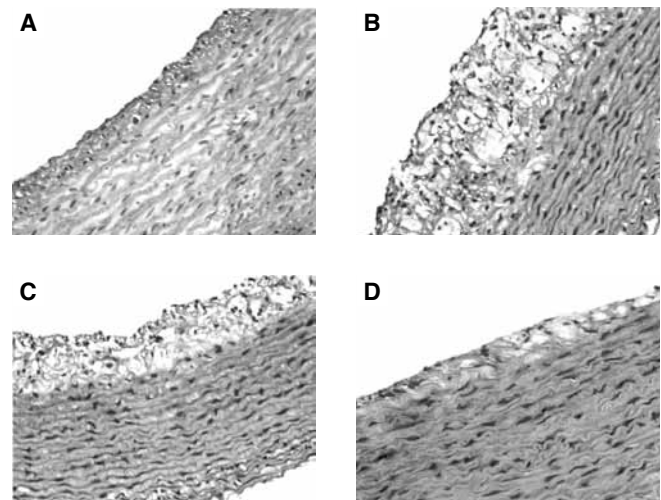


Fig. 1. Morphology of the aorta wall in the C (A), Zn (B), Ch (C) and Hm (D) groups. Except for the C and Hm groups, all other samples showed shedding of endothelial cells and the presence of foam cells. The tunica-intima was thickened and the smooth muscle layer was disorganised and extended towards the tunica-intima. (H&E staining, magnification 400 X).

TABLE 1. DETECTION OF SERUM LIPIDS, OX-LDL, NO AND ET-1

Groups	TC (mmol/l)	TG (mmol/l)	LDL-C (mmol/l)	HDL-C (mmol/l)	ox-LDL (μmol/l)	NO (μmol/l)	ET-1 (pg/ml)
C	1.70 ± 0.19	0.80 ± 0.15	0.80 ± 0.12	1.03 ± 0.33	1.34 ± 0.26	170.75 ± 2.25	113.88 ± 15.91
Zn	21.20 ± 1.89*	3.17 ± 1.16*	15.41 ± 2.74*	1.01 ± 0.20	2.68 ± 0.67*	121.49 ± 1.23*	198.12 ± 17.70**
Ch	21.66 ± 3.80*	3.05 ± 1.38*	15.31 ± 2.43*	1.10 ± 0.28	2.72 ± 0.65*	128.39 ± 0.94*	160.00 ± 15.32*
Hm	21.86 ± 2.32*	3.36 ± 1.80*	14.75 ± 2.33*	1.10 ± 0.30	2.63 ± 0.57*	129.19 ± 1.66*	127.68 ± 16.00**

Compared with the C group, * $p < 0.01$; compared with the Ch group, # $p < 0.01$.

TABLE 2. CO PRODUCTION, NO PRODUCTION AND NO ACTIVITY AND ET-1 IN AORTIC TISSUE (MEAN ± SD)

Groups	HbCO (nmol/mg.tissue)	NO ² (nmol/mg.protein)	CNOS (pmol.mg.protein ⁻¹ .min ⁻¹)	INOS (pmol.mg.protein ⁻¹ .min ⁻¹)	ET ¹ (pg/mg. tissue)
C	36.18 ± 3.59	120.21 ± 18.32	110.22 ± 10.84	97.28 ± 10.12	20.00 ± 3.89
Zn	16.85 ± 3.27**	88.73 ± 15.32*	63.87 ± 8.52**	169.92 ± 13.10**	64.43 ± 6.02**
Ch	56.09 ± 5.12*	87.86 ± 15.24*	62.01 ± 9.87*	144.40 ± 12.80*	42.78 ± 5.42*
Hm	79.21 ± 6.17**	86.22 ± 13.50*	63.12 ± 8.46*	120.96 ± 11.50**	30.23 ± 4.81*

Compared with the C group, * $p < 0.01$; compared with the Ch group, # $p < 0.01$.

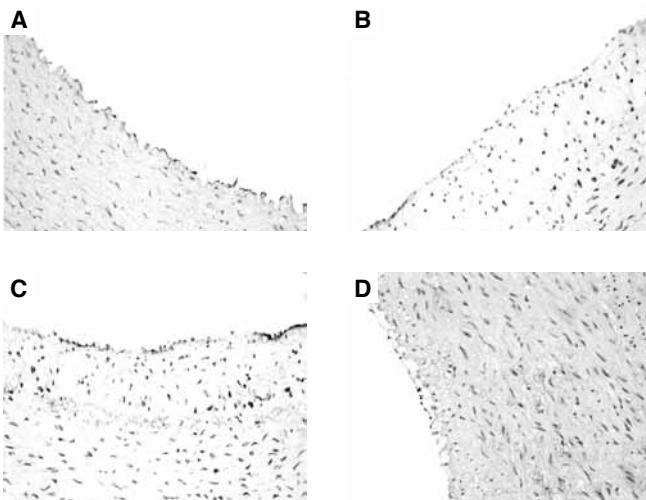


Fig. 2. Immunohistochemical detection in the C (A), Zn (B), Ch (C) and Hm (D) groups of the buffy lamellar particles of HO-1 present in the cytoplasm and cell membrane. HO-1 is mainly expressed by the endothelial, foam and smooth muscle cells of the tunica-intima (magnification 200 X).

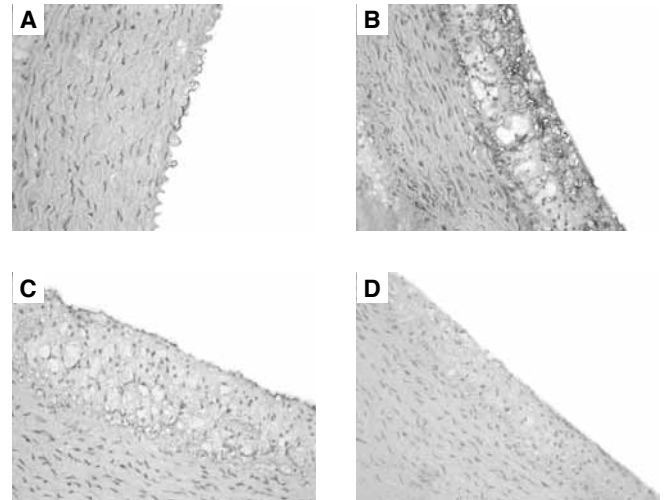


Fig. 3. Immunohistochemical detection in the C (A), Zn (B), Ch (C) and Hm (D) groups of ET-1. Buffy lamellar particles of ET-1 were located in the endothelial cells, foam cells and smooth muscle cells of the tunica-intima of the aorta (magnification 200 X).

In the Ch group, the density of positive cells was high, and HO-1 was expressed in the endothelial and foam cells in plaques. The expression rate of HO-1 was significantly higher than in the C group (40.98 ± 2.47 vs $19.02 \pm 1.28\%$, $p < 0.01$). In the Hm group, the density of positive cells was very high, and HO-1 was widely expressed in the endothelial and smooth muscle cells. The expression rate of HO-1 was significantly higher than in the Ch group (90.84 ± 6.42 vs $40.98 \pm 2.47\%$, $p < 0.01$).

As shown in Figs 3 and 4, the immunohistochemical staining and PCR of ET-1 showed that there was no obvious ET-1 expression in the aortic wall in the C group ($16.08 \pm 1.30\%$). The Zn and Ch groups showed strongly positive ET-1 expression (74.16 ± 4.28 , 59.28 ± 3.42 , vs $16.08 \pm 1.30\%$, $p < 0.01$), and the Hm group showed weakly positive expression (23.71 ± 1.49 vs $16.08 \pm 1.38\%$, $p < 0.01$).

mRNA expressions of HO-1 and ET-1 in aortic tissue

Compared with the C group, HO-1 mRNA expression in both the Ch and Hm groups was significantly increased (1.27 ± 0.16 , 1.61 ± 0.22 vs 1.06 ± 0.12 , all $p < 0.01$), especially in the Hm group with a 1.2-fold increase. HO-1 mRNA expression was significantly decreased in the Zn group (0.84 ± 0.15 vs 1.06 ± 0.12 , $p < 0.01$). Compared with the Ch group, HO-1 mRNA expression was significantly increased in the Hm group (1.61 ± 0.22 vs 1.27 ± 0.16 , $p < 0.01$).

The RT-PCR result showed that ET-1 mRNA expression in the Hm, Ch and Zn groups was significantly higher than in the C group (1.07 ± 0.09 , 1.59 ± 0.16 , 2.11 ± 0.25 vs 0.75 ± 0.15 , all $p < 0.01$). Compared with the Ch group, ET-1 mRNA expression was significantly decreased in the Hm group (1.07 ± 0.09 vs 1.59 ± 0.16 , $p < 0.01$), whereas ET-1 mRNA expres-

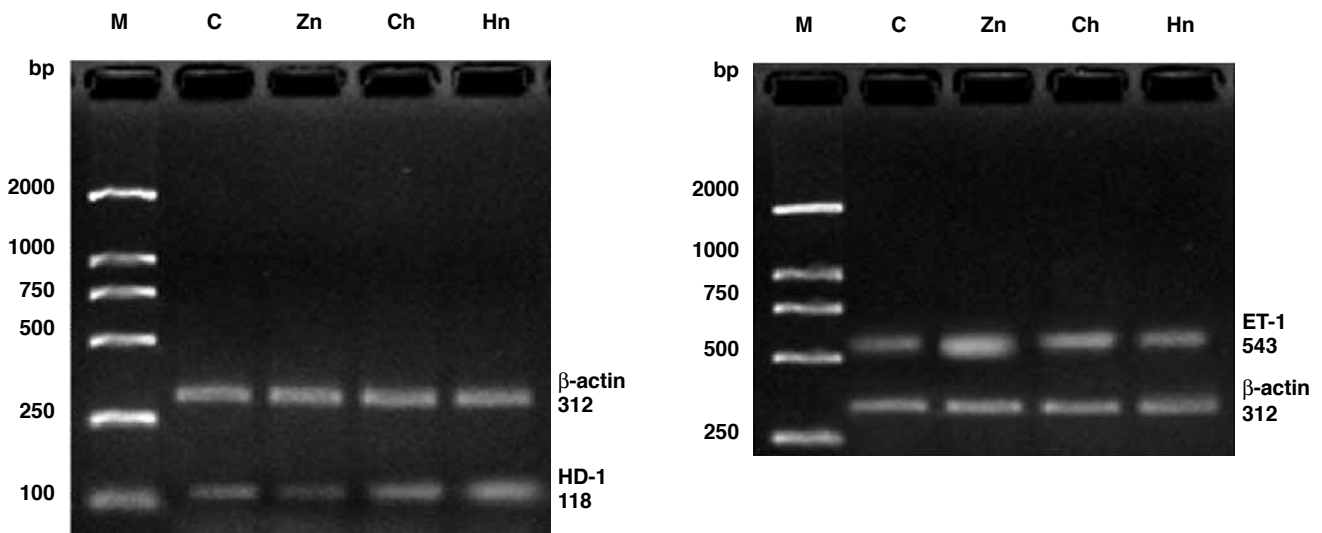


Fig. 4. Levels of HO-1 (left) and ET-1 (right) mRNA expression in the aorta. M: marker, C, Zn, Ch and Hm groups.

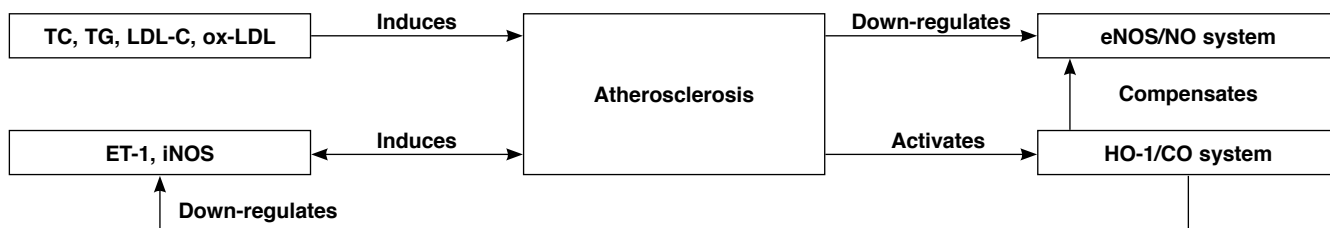


Fig. 5. Diagram showing the relationship between factors involved in atherosclerotic plaque formation.

sion in the Zn group was significantly increased (2.11 ± 0.25 vs 1.59 ± 0.16 , $p < 0.01$).

Discussion

Blood vessel endothelium is regulated by both NO-dependent and -independent vascular relaxing factors. Endogenous CO is an NO-independent vascular relaxing factor. CO and NO play complementary or equivalent physiological roles in the maintenance of normal physiological function of blood vessels.^{8,9} NO has 50-fold more affinity to cGMP than CO, therefore, NO plays the major role under physiological conditions.¹⁰ During the process of atherosclerosis development, the endothelial function is impaired. Therefore, the endothelium-derived cNOS expression or activity as well as the production of endothelial NO is decreased, whereas the activity of vascular smooth muscle cell (VSMC)-expressed iNOS is increased,^{11,12} resulting in increased NO free-radical production, which stimulates cell apoptosis and collagen degradation and promotes the development of atherosclerosis.^{11,13} NO free radicals could also synthesise peroxynitrite through a reaction with superoxide anion, thus causing further tissue damage.¹²

During the development of atherosclerosis, HO-1 shows inducible expression, and the production of CO is increased. On one hand, the activity and production of iNOS is inhibited and tissue damage is reduced.¹⁴ Possible mechanisms are based on the fact that iNOS contains a haeme domain, the latter a substrate of HO-1. (1) Increased activity of HO-1 therefore accelerates the degradation of iNOS. (2) An iNOS active site needs two haem molecules. The increased activity of HO-1 accelerates the degradation of haem and decreases iNOS synthesis. (3) CO combines with iNOS to make it inactive.¹⁵ (4) Free iron released during haeme decomposition further inhibits iNOS production by inhibiting nuclear transcription. Increased CO enhances cGMP levels, relaxes blood vessels and compensates for the insufficient functioning of endothelial cNOS producing NO.

The relationship between all factors involved in atherosclerotic plaque formation is shown in Fig. 5. Of significance is the decrease in cNOS expression and activity in the pathological condition. Our study showed that cNOS activity and NO production were significantly decreased in atherosclerotic aortic tissue. Simultaneously, HO-1 expression and activity and CO production were significantly increased. The area of aortic plaque in the Ch group was less than that in the Zn group. However, in the Zn group, the HO activity and expression and CO production were significantly decreased, the iNOS activity was significantly increased, and the area of aortic plaque was the largest. This suggests that the NOS/NO system was inhibited during the atherosclerotic process, and that the HO/CO system had a compensatory protective effect.

The HO inhibitor Znpp-IX could reduce the compensation of

the HO/CO system, thereby aggravating atherosclerosis. It can be seen that the NOS/NO and HO/CO systems had regulatory and compensatory effects on each other during the atherosclerotic process. The HO/CO system inhibited atherosclerotic progression through the regulation and compensation for NOS and NO. Therefore, the effect of the HO/CO system is more important in pathological conditions such as atherosclerosis.

VSMCs proliferation is an important pathological feature of atherosclerosis. ET-1 stimulates pro-oncogene expressions of c-myc and c-fos and DNA synthesis in vascular smooth muscle cells in a dose-dependent manner through strong and long-lasting vasoconstrictor effects, thereby promoting the proliferation of VSMCs and participating in the formation of atherosclerosis.¹⁶ With the co-culture of endothelial cells and VSMCs, Morita *et al.*⁶ found that HO-1 mRNA expression was increased in hypoxic VSMCs, and that hypoxic VSMCs could inhibit the high expression of ET-1 and PDGF-B mRNA and the secretion of ET-1 in hypoxia-induced human umbilical vein endothelial cells. This effect may be removed by the strong HO inhibitor, ZnPP-IX, and also by the CO scavenger, haemoglobin. Therefore, it is thought that VSMC-derived CO could inhibit the expressions of ET-1 and PDGF-B in endothelial cells via paracrine factors, thereby further inhibiting the self-proliferation of VSMCs.

Conclusion

In our study, after interference with atherosclerotic plaque formation by the HO inducer, haemin, HO-1 activity was significantly increased, HO-1 mRNA and protein expression were significantly increased, and CO generation also increased significantly, whereas the ET-1 level and expressions of ET-1 mRNA and protein were significantly reduced compared to all other groups. The area of aortic plaque was significantly decreased, indicating that the progression of atherosclerosis was effectively inhibited. The inhibitory effect of haemin on ET-1 expression may have been related to the inhibition of HO-1 on the cytochrome P450 mono-oxygenase, on which ET-1 synthesis depends. ET-1 expression is related to VSMCs proliferation. Therefore the anti-atherogenic target of the HO-1/CO system is further identified.

Our study indicated that the HO-1/CO system had anti-atherosclerotic effects, which were not achieved through its regulation of serum lipids or ox-LDL but was probably related to regulation and compensation of the NOS/NO system and down-regulation of ET-1 expression.

This work was supported by the National Science Foundation of China (No. 39800065) the National Science Foundation of Guizhou Province (No. 2006-2074), and the Shengzhang Fund of Excellent Technological and Educational Talents of Guizhou Province (No.2007-72). We thank Mr Qianglin Duan, a skilled English proof-reader from Tongji Hospital, for language editing and article revision.

References

1. Tulis DA, Durante W, Peyton KJ, *et al.* Heme oxygenase-1 attenuates vascular remodeling following balloon injury in rat carotid arteries. *Atherosclerosis* 2001; **155**: 113–122.
2. Togane Y, Morita T, Suematsu M, *et al.* Protective roles of endogenous carbon monoxide in neointimal development elicited by arterial injury. *Am J Physiol Heart Circ Physiol* 2000; **278**: H623–632.
3. Christodoulides N, Durante W, Kroll MH, *et al.* Vascular smooth muscle cell heme oxygenases generate guanylyl cyclase stimulatory carbon monoxide. *Circulation* 1995; **91**: 2306–2309.
4. Beltowski J, Jamroz A, Borkowska E. Heme oxygenase and carbon monoxide in the physiology and pathology of the cardiovascular system. *Postepy Hig Med Dosw* 2004; **58**: 83–99.
5. Green LC, Wagner DA, Glogowski J, *et al.* Analysis of nitrate, nitrite and [¹⁵N] nitrate in biological fluids. *Anal Biochem* 1982; **126**: 131–138.
6. Morita T, Kourembanas S. Endothelial cell expression of vasoconstrictors and growth factors is regulated by smooth muscle cell-derived carbonmonoxide. *J Clin Invest* 1995; **96**: 2676–2682.
7. Wang XB, Huang HL, Zhang LZ, *et al.* Detection and application of nitric oxide synthase. *J Beijing Med Univ* 1994; **26**: 173–176.
8. Ryter SW, Morse D, Choi AM. Carbon monoxide: to boldly go where NO has gone before. *Sci STKE* 2004; **230**: RE6.
9. Johnson FK, Teran FJ, Prieto-Carrasquero M, *et al.* Vascular effects of a heme oxygenase inhibitor are enhanced in the absence of nitric oxide. *Am J Hypertens* 2002; **15**: 1074–1080.
10. Siow RC, Sato H, Mann GE. Heme oxygenase-carbon monoxide signaling pathway in atherosclerosis: anti-atherogenic actions of bilirubin and carbon monoxide? *Cardiovasc Res* 1999; **41**: 385–394.
11. Cromheeke KM, Kockx MM, DeMeyer GR, *et al.* Inducible nitric oxide synthase colocalizes with signs of lipid oxidation/peroxidation in human atherosclerotic plaques. *Cardiovasc Res* 1999; **43**: 744–754.
12. Stasch JP, Schmidt PM, Nedvetsky PI, *et al.* Targeting the heme-oxidized nitric oxide receptor for selective vasodilatation of diseased blood vessels. *J Clin Invest* 2006; **116**: 2552–2561.
13. Cheng ZW, Zhu WL. Study of the relationship between asymmetric dimethylarginine and coronary atherosclerotic heart disease. *Chin J Cardiol* 2004; **32**: 312–324.
14. Yang NC, Lu LH, Kao YH, *et al.* Heme oxygenase-1 attenuates interleukin-1beta-induced nitric oxide synthase expression in vascular smooth muscle cells. *J Biomed Sci* 2004; **11**: 799–809.
15. Hartsfield CL. Cross talk between carbon monoxide and nitric oxide. *Antioxid Redox Signal* 2002; **4**: 301–307.
16. Nagata N, Niwa Y, Nakaya Y. A novel 31-amino-acid-length endothelin, ET-1(1-31), can act as a biologically active peptide for vascular smooth muscle cells. *Biochem Biophys Res Commun* 2000; **275**: 595–600.

Letter to the Editor

Dear Sir

Commenting on the article ‘Cerebral embolism following thrombolytic therapy for acute myocardial infarction: the second reported case’ by M Bostan, *et al.*,¹ I note that the captions for Figs 1 and 2 are reversed. I would also like to comment on the description of the second brain CT performed on the patient presented in this case report.

The authors report that after two hours of intravenous thrombolytic therapy (TT) administration, a brain CT was performed on the patient, which showed ‘no pathological abnormality’. They state that in the second brain CT 12 hours later ‘extensive infarction of the left frontal area was seen (Fig. 2)’.

Careful examination of this second brain CT (Fig. 2) shows that the pathology was not as homogeneous as portrayed and reveals (1) a darker parasagittal, medial wedge-shaped lesion, suggesting an ‘older’ infarct in the territory of the anterior cerebral artery (ACA), and (2) effacement of the left frontal sulci and gyri, as well as blurring of the gray/white matter interface, suggesting oedema, which could be related to a recent, acute ischaemia within the territory of the left middle cerebral artery (MCI).

Without the benefit of the images of the first brain CT (which was described as normal), it is difficult to be more categorical. However, the image of the second brain CT (Fig. 2) suggests that there might have been two different ischaemic events, (1) an older left parasagittal infarct within the vascular territory of the ACA, already showing signs of encephalomalacia, and

(2) a larger oedema of the left frontal lobe, suggesting a recent, acute cerebrovascular incident within the vascular territory of the MCA.

Older patients (such as the one described in this case report) who are at a higher risk of potentially life-threatening vascular disease should be carefully evaluated (within the short time frame for decision making) before instituting TT to restore antegrade flow of an acutely occluded coronary artery, or alternatively, be treated by percutaneous coronary intervention (PCI). Attention to detail will hopefully avert a third case report, while remembering that the doctor’s most basic tenet is: ‘primum non nocere’ – first, do no harm.

To elucidate this diagnostic interpretation of the second brain CT (Fig. 2), I would appreciate the comments of the authors of this case report and especially of the radiologist(s) who performed the first brain CT, who have the benefit of being able to compare both brain scans.

MARIO P ITURRALDE, marionuclear@yebo.co.za
Emeritus Professor of Nuclear Medicine (retired)
University of Pretoria

Reference

1. Bostan, M, Kanat A, Sen M, Kazdal H, Bostan H. Cerebral embolism following thrombolytic therapy for acute myocardial infarction: the second case report. *Cardiovasc J Afr* 2010; **21**: 155–157.